SCIENCE CHINA
Information Sciences

• RESEARCH PAPERS •
Special Focus

February 2010 Vol. 53 No. 2: 248–257
doi: 10.1007/s11432-010-0035-7

Research on network RTK positioning algorithm aided by quantum ranging

YANG ChunYan*, WU DeWei, LU YanE & YU YongLin

The Telecommunication Engineering Institutes, Air Force Engineering University, Xi'an 710077*, China*

Received July 24, 2009; accepted December 29, 2009

Abstract It is well-known that the integer ambiguities of network real time kinematics (RTK) in GPS can hardly be precisely resolved because of the small change of position dilution of precision (PDOP) within a few observation epochs. In response to this, an integer ambiguities resolution method aided by the high precision quantum ranging is proposed, in which the Householder transformation is employed to preserve the independence of different observations. Consequently, the reliability of the integer ambiguities' floating solution is improved mathematical analysis and simulation experiment are conducted to validate the effectiveness of the proposed method.

Keywords quantum ranging, network RTK, Householder transformation, PDOP

Citation Yang C Y, Wu D W, Lu Y E, et al. Research on network RTK positioning algorithm aided by quantum ranging. Sci China Inf Sci, 2010, 53: 248–257, doi: 10.1007/s11432-010-0035-7

1 Introduction

Satellite navigation is a hot topic in the field of high-precision radio navigation. Some key problems related to it such as carrier phase integer ambiguities resolution, cycle slip detection and repair, have now been resolved. Short baseline real time kinematics (RTK) has achieved very high positioning accuracy. RTK receivers have been widely used in real time high-precision navigation, survey and mapping. For instance, the advanced RTK receivers of NovAtle Co. can provide real-time, robust and reliable positioning with centimeter-level accuracy when the baseline distance is less than 40 km [1]. In the meantime, the dynamic range of the user's speed can be up to 520 m/s. If multiple reference stations are properly integrated to form a network RTK, the limitation of baseline distance on positioning accuracy can be further reduced [2]. However, carrier phase integer ambiguity resolution is still the key issue to network RTK. Most of the existing resolution methods are based on double differenced method, which has the advantage of definite physical meaning. But the original data in the same epoch are not independent of each other. As a result, integer ambiguities cannot be determined accurately [3]. Up to now, different techniques have been proposed for the decorrelation of the integer ambiguities. Least-squares ambiguity decorrelation adjustment (LAMBDA) method presented by Teunissen [4] can solve an integer least squares (ILS) problem to obtain the estimations of the double differenced integer ambiguities, but it may not be suitable for real time applications with high dimensions because its computation time is relatively long.

*Corresponding author (email: ycy220@163.com)

The modified LAMBDA (MLAMBDA) method can improve the computational efficiency, but it does not improve the accuracy and reliability of integer ambiguities resolution [5].

Quantum positioning system (QPS) using entangled and squeezed quantum pulse is a newly developed positioning technology in recent years. Higher positioning accuracy can be achieved because it can overcome classical power/bandwidth limitations. Many research institutes, such as Massachusetts Institute of Technology (MIT) and Army Research Laboratory (ARL) in US are paying great attentions to it [6–10]. Considering that it may be impossible to build a complete set of QPS within a short period of time to replace satellite navigation system, high-precision network RTK should still play a primary role in the near future. So the integration of network RTK and QPS shows good prospect. This paper addresses the way to integrate the quantum ranging technique of QPS with the existing network RTK to improve the reliability of integer ambiguities resolution within a few observation epochs.

2 The integer ambiguities resolution aided by quantum ranging

2.1 The mathematical model

To apply the new approach with the aid of quantum ranging, integer ambiguities resolution in network RTK should be introduced. Without loss of generality, an example related to GPS is taken to explain the principle.

The positioning equations of both code and carrier phase measurements of GPS can be respectively given by

$$\phi_v^i(k) = \rho_v^i(k) - I_v^i(k) + T_v^i(k) + N_v^i + \delta t_v(k) - \delta t_v^i(k) + D_v(k) - D^i(k) + \phi_v - \phi^i + \eta_v^i(k), \tag{1}$$

$$\tilde{\rho}_v^i(k) = \rho_v^i(k) + I_v^i(k) + T_v^i(k) + \delta t_v(k) - \delta t^i(k) + d_v(k) - d^i(k) + \zeta_v^i(k), \tag{2}$$

$\phi_v^i(k)$: the carrier phase measurement at epoch k.
$\tilde{\rho}_v^i(k)$: the code measurement at epoch k.
$\rho_v^i(k)$: the real range between virtual reference station (VRS) and satellite i.
$I_v^i(k)$: the ionospheric range error at epoch k.
$T_v^i(k)$: the tropospheric range error at epoch k.
N_v^i: the integer ambiguity.
$\delta t_v(k)$: the virtual reference station clock error at epoch k.
$\delta t_v^i(k)$: the satellite clock error at epoch k.
$D_v(k)$: the virtual reference station's hardware delay for carrier-phase measurement.
$D^i(k)$: the satellite hardware delay for carrier-phase measurement.
$d_v(k)$: the virtual reference station's hardware delay for code measurement.
$d^i(k)$: the satellite hardware delay for code measurement.
ϕ_v: the initial phase of the satellite generated carrier signal at the initial time.
ϕ^i: the initial phase of the VRS generated carrier signal at the initial time.
$\eta_v^i(k)$: the carrier phase measurement noise, including multipath error.
$\zeta_v^i(k)$: the code measurement noise, including multipath noise.

It can be assumed that $\eta_v^i(k)$ is the Gaussian noise with zero mean and σ_ϕ^2 variance, and $\zeta_v^i(k)$ is the Gaussian noise with zero mean and σ_ρ^2 variance.

For the mobile station, the subscript of above equations v can be replaced by r, and then the corresponding phase and code observation equations are given by

$$\phi_r^i(k) = \rho_r^i(k) - I_r^i(k) + T_r^i(k) + N_r^i + \delta t_r(k) - \delta t_r^i(k) + D_r(k) - D^i(k) + \phi_r - \phi^i + \eta_r^i(k), \tag{3}$$

$$\tilde{\rho}_r^i(k) = \rho_r^i(k) + I_r^i(k) + T_r^i(k) + \delta t_r(k) - \delta t^i(k) + d_r(k) - d^i(k) + \zeta_r^i(k). \tag{4}$$

Since the baseline is short, we have

$$-[I_v^i(k) - I_r^i(k)] + [T_v^i(k) - T_r^i(k)] - [\delta t_v^i(k) - \delta t_r^i(k)] - [D^i(k) - D^i(k)] - [\phi^i - \phi^i] \approx 0. \tag{5}$$

Thus by defining

$$\phi_k^i \triangleq \phi_v^i(k) - \phi_r^i(t_k), \quad \rho_k^i \triangleq \rho_v^i(k) - \rho_r^i(k), \quad N^i \triangleq N_v^i - N_r^i, \quad \eta_k^i \triangleq \eta_v^i(k) - \eta_r^i(k),$$
$$\beta_k^\phi \triangleq \delta t_v(k) - \delta t_r(k) + D_v(k) - D_r(k) + \phi_v - \phi_r,$$
$$\tilde{\rho}_k^i \triangleq \tilde{\rho}_v^i(k) - \tilde{\rho}_r^i(k), \quad \zeta_k^i \triangleq \zeta_v^i(k) - \zeta_r^i(k),$$
$$\beta_k^\rho \triangleq \delta t_v(k) - \delta t_r(k) + d_v(k) - d_r(k),$$

the single differenced carrier phase and code measurement equations can be obtained by subtracting eq. (3) from eq. (1) and eq. (4) from eq. (2) respectively,

$$\phi_k^i = \rho_k^i + N^i + \beta_k^\phi + \eta_k^i, \tag{6}$$
$$\tilde{\rho}_k^i = \rho_k^i + \beta_k^\rho + \zeta_k^i. \tag{7}$$

Due to

$$\begin{cases} \rho_v^i(k) = \{[x^i(k) - x_v(k)]^2 + [y^i(k) - y_v(k)]^2 + [z^i(k) - z_v(k)]^2\}^{1/2}, \\ \rho_r^i(k) = \{[x^i(k) - x_r(k)]^2 + [y^i(k) - y_r(k)]^2 + [z^i(k) - z_r(k)]^2\}^{1/2}, \end{cases}$$

$\rho_v^i(k)$ and $\rho_r^i(k)$ can be linearized by using the first-order Taylor series expansion at $\{x_0(k), y_0(k), z_0(k)\}$ as

$$\rho_k^i = [\Delta\rho_v^i(k) - \Delta\rho_r^i(k)] + \frac{x_0(k) - x^i(k)}{\rho_0^i(k)}[x_r(k) - x_v(k)] + \frac{y_0(k) - y^i(k)}{\rho_0^i(k)}[y_r(k) - y_v(k)]$$
$$+ \frac{z_0(k) - z^i(k)}{\rho_0^i(k)}[z_r(k) - z_v(k)], \tag{8}$$

where

$$\rho_0^i(k) = \sqrt{[x^i(k) - x_0(k)]^2 + [y^i(k) - y_0(k)]^2 + [z^i(k) - z_0(k)]^2},$$

$\Delta\rho_v^i(k)$ denotes the difference between pseudo-range observation $\tilde{\rho}_v^i(k)$ and its theoretical value. $\Delta\rho_r^i(k)$ represents the difference between pseudo-range measurement $\tilde{\rho}_r^i(k)$ and its theoretical value.

If eq. (8) is substituted into eqs. (6) and (7), we have

$$\phi_k^i = [\Delta\rho_v^i(k) - \Delta\rho_r^i(k)] + \frac{x_0(k) - x^i(k)}{\rho_0^i(k)}[x_r(k) - x_v(k)] + \frac{y_0(k) - y^i(k)}{\rho_0^i(k)}[y_r(k) - y_v(k)]$$
$$+ \frac{z_0(k) - z^i(k)}{\rho_0^i(k)}[z_r(k) - z_v(k)] + N^i + \beta_k^\phi + \eta_k^i, \tag{9}$$
$$\tilde{\rho}_k^i = [\Delta\rho_v^i(k) - \Delta\rho_r^i(k)] + \frac{x_0(k) - x^i(k)}{\rho_0^i(k)}[x_r(k) - x_v(k)] + \frac{y_0(k) - y^i(k)}{\rho_0^i(k)}[y_r(k) - y_v(k)]$$
$$+ \frac{z_0(k) - z^i(k)}{\rho_0^i(k)}[z_r(k) - z_v(k)] + \beta_k^\rho + \zeta_k^i. \tag{10}$$

For m visible satellites, it can be assumed that satellite 1 is the reference satellite with the biggest elevation angle. And this will not lose any generality. So eqs. (9) and (10) can be rewritten in matrix form as

$$\boldsymbol{\Phi}_k = \boldsymbol{\Gamma}_k + \boldsymbol{A}_k \boldsymbol{X}_k + \boldsymbol{N} + \boldsymbol{\beta}_k^\phi + \boldsymbol{\eta}_k, \tag{11}$$

where

$$\boldsymbol{\Phi}_k = \begin{bmatrix} \phi_k^1 \\ \phi_k^2 \\ \vdots \\ \phi_k^m \end{bmatrix}, \quad \boldsymbol{\Gamma}_k = \begin{bmatrix} \Delta\rho_v^1(k) - \Delta\rho_r^1(k) \\ \Delta\rho_v^2(k) - \Delta\rho_r^2(k) \\ \vdots \\ \Delta\rho_v^m(k) - \Delta\rho_r^m(k) \end{bmatrix}, \quad \boldsymbol{A}_k = \begin{bmatrix} \frac{x_0(k)-x^1(k)}{\rho_0^1(k)} & \frac{y_0(k)-y^1(k)}{\rho_0^1(k)} & \frac{z_0(k)-z^1(k)}{\rho_0^1(k)} \\ \frac{x_0(k)-x^2(k)}{\rho_0^2(k)} & \frac{y_0(k)-y^2(k)}{\rho_0^2(k)} & \frac{z_0(k)-z^2(k)}{\rho_0^2(k)} \\ \vdots & \vdots & \vdots \\ \frac{x_0(k)-x^m(k)}{\rho_0^m(k)} & \frac{y_0(k)-y^m(k)}{\rho_0^m(k)} & \frac{z_0(k)-z^m(k)}{\rho_0^m(k)} \end{bmatrix},$$

$$\boldsymbol{X}_k = \begin{bmatrix} x_r(k) - x_v(k) \\ y_r(k) - y_v(k) \\ z_r(k) - z_v(k) \end{bmatrix}, \quad \boldsymbol{N} = \begin{bmatrix} N^1 \\ N^2 \\ \vdots \\ N^m \end{bmatrix}, \quad \boldsymbol{\beta}_k^{\phi} = \begin{bmatrix} \beta_k^{\phi} \\ \beta_k^{\phi} \\ \vdots \\ \beta_k^{\phi} \end{bmatrix}, \quad \boldsymbol{\eta}_k = \begin{bmatrix} \eta_k^1 \\ \eta_k^2 \\ \vdots \\ \eta_k^m \end{bmatrix}, \quad \boldsymbol{\eta}_k \sim \mathcal{N}(\boldsymbol{0}, \sigma_{\phi}^2 \boldsymbol{I}_m),$$

and

$$\boldsymbol{\rho}_k = \boldsymbol{\Gamma}_k + \boldsymbol{A}_k \boldsymbol{X}_k + \boldsymbol{\beta}_k^{\rho} + \boldsymbol{\zeta}_k, \tag{12}$$

where

$$\boldsymbol{\rho}_k = \begin{bmatrix} \rho_k^1 \\ \rho^2 \\ \vdots \\ \rho_k^m \end{bmatrix}, \quad \boldsymbol{\beta}_k^{\rho} = \begin{bmatrix} \beta_k^{\rho} \\ \beta_k^{\rho} \\ \vdots \\ \beta_k^{\rho} \end{bmatrix}, \quad \boldsymbol{\zeta}_k = \begin{bmatrix} \zeta_k^1 \\ \zeta_k^2 \\ \vdots \\ \zeta_k^m \end{bmatrix}, \quad \boldsymbol{\zeta}_k \sim \mathcal{N}(\boldsymbol{0}, \sigma_{\rho}^2 \boldsymbol{I}_m).$$

In GPS positioning, the single differenced error terms are independent of each other, but the double differenced terms are correlate with each other. Instead of the popular double differenced technique, the Householder transformation can be employed to ensure that the transformed measurements are still uncorrelated [4].

2.2 Householder transformation

Define the matrix

$$\bar{\boldsymbol{P}} = \left[\frac{\boldsymbol{e}}{\sqrt{m}}, \boldsymbol{I}_{m-1} - \frac{\boldsymbol{e}\boldsymbol{e}^{\mathrm{T}}}{m - \sqrt{m}} \right] = \boldsymbol{F}\boldsymbol{J}, \tag{13}$$

where $\bar{\boldsymbol{P}}$ denotes an $m \times m$ Householder matrix with the exclusion of the first row. $\boldsymbol{I}_{m-1}$ represents a $(m-1) \times (m-1)$ unit matrix and $\boldsymbol{e} = [1, 1, \ldots, 1]^{\mathrm{T}}$. Also, we can define

$$\begin{cases} \boldsymbol{F} = \boldsymbol{I}_{m-1} - \dfrac{\boldsymbol{e}\boldsymbol{e}^{\mathrm{T}}}{m - \sqrt{m}}, \\ \boldsymbol{J} = [-\boldsymbol{e}, \boldsymbol{I}_{m-1}]. \end{cases}$$

Then

$$\begin{cases} \bar{\boldsymbol{P}}\boldsymbol{\beta}_k^{\phi} = \boldsymbol{0}, \\ \bar{\boldsymbol{P}}\boldsymbol{\beta}_k^{\rho} = \boldsymbol{0}, \end{cases} \tag{14}$$

and

$$\bar{\boldsymbol{P}}\boldsymbol{N} = \boldsymbol{F}\boldsymbol{J}\boldsymbol{N} = \boldsymbol{F}\boldsymbol{Z}, \tag{15}$$

where $\boldsymbol{Z} = [N^2 - N^1, N^3 - N^1, \ldots, N^m - N^1]^{\mathrm{T}}$ denotes the double differenced integer ambiguity (DDIA) vector.

Left-multiplying eqs. (11) and (12) by $\bar{\boldsymbol{P}}$ respectively, we can obtain

$$\bar{\boldsymbol{P}}\boldsymbol{\Phi}_k = \bar{\boldsymbol{P}}\boldsymbol{\Gamma}_k + \bar{\boldsymbol{P}}\boldsymbol{A}_k\boldsymbol{X}_k + \boldsymbol{F}\boldsymbol{Z} + \bar{\boldsymbol{P}}\boldsymbol{\eta}_k, \tag{16}$$

$$\bar{\boldsymbol{P}}\boldsymbol{\eta}_k \sim \mathcal{N}(\boldsymbol{0}, \sigma_{\phi}^2 \boldsymbol{I}_{m-1}),$$

$$\bar{\boldsymbol{P}}\boldsymbol{\rho}_k = \bar{\boldsymbol{P}}\boldsymbol{\Gamma}_k + \bar{\boldsymbol{P}}\boldsymbol{A}_k\boldsymbol{X}_k + \bar{\boldsymbol{P}}\boldsymbol{\zeta}_k, \tag{17}$$

$$\bar{\boldsymbol{P}}\boldsymbol{\zeta}_k \sim \mathcal{N}(\boldsymbol{0}, \sigma_{\rho}^2 \boldsymbol{I}_{m-1}).$$

For different epochs, it can be assumed that the total number of epochs is K and the time interval between the adjacent epochs is 1 s. The variation of GPS related to the user's position dilution of precision (PDOP) is small within a few epochs. In this case, the positioning accuracy cannot be improved obviously with the increase of epochs [11]. Therefore, the pseudo-range observation at epoch $k-1$ is smoothed through the carrier phase observation before further positioning processing in this paper. And the computation burden can be reduced effectively without the dilution of the positioning precision.

The specific steps are given as follows:

ϕ_k^i denotes the ith component of $\boldsymbol{\Phi}_k$ in eq. (16), and ρ_k^i denotes the ith component of $\boldsymbol{\rho}_k$ in eq. (17). Also, ρ_k^i at epoch k can be estimated by just using the mean of previous $k-1$ epoch observations

$$\hat{\rho}_k^i = \bar{\rho}_{k-1}^i + \phi_k^i - \phi_{k-1}^i, \tag{18}$$

where $\bar{\rho}_{k-1}^i$ is the smoothed pseudo-range at epoch $k-1$ and $\hat{\rho}_k^i$ is the estimated pseudo-range at epoch k. If the pseudo-range observation at epoch k is also taken into consideration, then we can get

$$\bar{\rho}_k^i = \frac{1}{k}\rho_k^i + \frac{k-1}{k}\hat{\rho}_k^i, \tag{19}$$

where $\bar{\rho}_k^i$ and ρ_k^i are the smoothed pseudo-range and observation pseudo-range at epoch k respectively. And the initial condition of this process can be given by $\hat{\rho}_1^i = \rho_1^i$. Now all the elements of $\boldsymbol{\rho}_k$'s smoothed value in eq. (17) can be obtained by using both eqs. (18) and (19). Notice that eqs. (18) and (19) are used in scalar form such that the computational complexity is reduced. And this is good for real-time processing. Due to $\sigma_\phi \ll \sigma_\rho$, each component of $\bar{\boldsymbol{\rho}}_{K-1}$ is approximately proportional to the inverse of the smoothing epoch number, when the smoothing epoch number in document is small. So its covariance matrices can be written as

$$\mathrm{cov}(\bar{\boldsymbol{\rho}}_{K-1}) \approx \frac{1}{K-1}\sigma_\rho^2 I_{m-1}. \tag{20}$$

Define $\sigma = \sigma_\phi/\sigma_\rho$, $\sigma' = \sqrt{K-1}\sigma_\phi/\sigma_\rho$. From eqs. (16)–(20), it follows that

$$\begin{bmatrix} \sigma'\bar{\boldsymbol{P}}\bar{\boldsymbol{\rho}}_{K-1} \\ \sigma\bar{\boldsymbol{P}}\rho_K \\ \bar{\boldsymbol{P}}\boldsymbol{\Phi}_K \end{bmatrix} = \boldsymbol{H}_{K-1,K} + \begin{bmatrix} \boldsymbol{0} \\ \boldsymbol{0} \\ \boldsymbol{I}_{m-1} \end{bmatrix} \boldsymbol{F}\boldsymbol{Z} + \begin{bmatrix} \sigma'\bar{\boldsymbol{P}}\boldsymbol{\zeta}'_{K-1} \\ \sigma\bar{\boldsymbol{P}}\zeta_K \\ \bar{\boldsymbol{P}}\boldsymbol{\eta}_K \end{bmatrix}, \begin{bmatrix} \sigma'\bar{\boldsymbol{P}}\zeta'_{K-1} \\ \sigma\bar{\boldsymbol{P}}\zeta_K \\ \bar{\boldsymbol{P}}\eta_K \end{bmatrix} \sim \mathcal{N}(\boldsymbol{0}, \sigma_\varphi^2 \boldsymbol{I}_{3m-3}), \tag{21}$$

where

$$\boldsymbol{H}_{K-1,K} = \begin{bmatrix} \sigma'\bar{\boldsymbol{P}}\boldsymbol{\Gamma}_{K-1} + \sigma'\bar{\boldsymbol{P}}\boldsymbol{A}_{K-1}\boldsymbol{X}_{K-1} \\ \sigma\bar{\boldsymbol{P}}\boldsymbol{\Gamma}_K + \sigma\bar{\boldsymbol{P}}\boldsymbol{A}_K\boldsymbol{X}_K \\ \bar{\boldsymbol{P}}\boldsymbol{\Gamma}_K + \bar{\boldsymbol{P}}\boldsymbol{A}_K\boldsymbol{X}_K \end{bmatrix}$$

and $\mathrm{rank}(\boldsymbol{H}_{K-1,K}) = m-1$. QR factorization of $\boldsymbol{H}_{K-1,K}$ can be written as

$$\boldsymbol{H}_{K-1,K} = \boldsymbol{H}_Q^{\mathrm{T}}\boldsymbol{H}_R, \tag{22}$$

where $\boldsymbol{H}_Q$ is a $(3m-3)\times(3m-3)$ orthogonal matrix, and $\boldsymbol{H}_R = [\boldsymbol{H}_{RR}^{\mathrm{T}}, \boldsymbol{0}]^{\mathrm{T}}$. $\boldsymbol{H}_{RR}$ is a $(2m-2)\times(3m-3)$ nonsingular upper triangular matrix, and $\mathrm{rank}(\boldsymbol{H}_{RR}) = m-1$. $\boldsymbol{H}_Q = [\tilde{\boldsymbol{H}}_Q^{\mathrm{T}}, \bar{\boldsymbol{H}}_Q^{\mathrm{T}}]^{\mathrm{T}}$. $\tilde{\boldsymbol{H}}_Q$ is a $(2m-2)\times(3m-3)$ matrix and $\bar{\boldsymbol{H}}_Q$ is an $(m-1)\times(3m-3)$ matrix. Left-multiplying eq. (21) by $\boldsymbol{H}_Q$, we have

$$\begin{bmatrix} \tilde{\boldsymbol{H}}_1 \\ \bar{\boldsymbol{H}}_2 \end{bmatrix} = \begin{bmatrix} \boldsymbol{H}_{RR} \\ \boldsymbol{0} \end{bmatrix} + \begin{bmatrix} \tilde{\boldsymbol{H}}_3 \\ \bar{\boldsymbol{H}}_4 \end{bmatrix} \boldsymbol{Z} + \begin{bmatrix} \tilde{\boldsymbol{H}}_5 \\ \bar{\boldsymbol{H}}_6 \end{bmatrix}, \tag{23}$$

$$\tilde{\boldsymbol{H}}_5 \sim \mathcal{N}(\boldsymbol{0}, \sigma_\varphi^2 \boldsymbol{I}_{2m-2}), \bar{\boldsymbol{H}}_6 \sim \mathcal{N}(\boldsymbol{0}, \sigma_\varphi^2 \boldsymbol{I}_{m-1}),$$

where

$$\tilde{\boldsymbol{H}}_1 = \tilde{\boldsymbol{H}}_Q \begin{bmatrix} \sigma'\bar{\boldsymbol{P}}\bar{\boldsymbol{\rho}}_{K-1} \\ \sigma\bar{\boldsymbol{P}}\boldsymbol{\rho}_K \\ \bar{\boldsymbol{P}}\boldsymbol{\Phi}_K \end{bmatrix}, \quad \bar{\boldsymbol{H}}_2 = \bar{\boldsymbol{H}}_Q \begin{bmatrix} \sigma'\bar{\boldsymbol{P}}\bar{\boldsymbol{\rho}}_{K-1} \\ \sigma\bar{\boldsymbol{P}}\boldsymbol{\rho}_K \\ \bar{\boldsymbol{P}}\boldsymbol{\Phi}_K \end{bmatrix}, \quad \tilde{\boldsymbol{H}}_3 = \tilde{\boldsymbol{H}}_Q \begin{bmatrix} \boldsymbol{0} \\ \boldsymbol{0} \\ \boldsymbol{I}_{m-1} \end{bmatrix} \boldsymbol{F},$$

$$\bar{\boldsymbol{H}}_4 = \bar{\boldsymbol{H}}_Q \begin{bmatrix} \boldsymbol{0} \\ \boldsymbol{0} \\ \boldsymbol{I}_{m-1} \end{bmatrix} \boldsymbol{F}, \quad \tilde{\boldsymbol{H}}_5 = \tilde{\boldsymbol{H}}_Q \begin{bmatrix} \sigma'\bar{\boldsymbol{P}}\boldsymbol{\zeta}'_{K-1} \\ \sigma\bar{\boldsymbol{P}}\zeta_K \\ \bar{\boldsymbol{P}}\boldsymbol{\eta}_K \end{bmatrix}, \quad \bar{\boldsymbol{H}}_6 = \bar{\boldsymbol{H}}_Q \begin{bmatrix} \sigma'\bar{\boldsymbol{P}}\boldsymbol{\zeta}'_{K-1} \\ \sigma\bar{\boldsymbol{P}}\zeta_K \\ \bar{\boldsymbol{P}}\boldsymbol{\eta}_K \end{bmatrix}.$$

From the lower part of eq. (23), we can obtain

$$\bar{\boldsymbol{H}}_2 = \bar{\boldsymbol{H}}_4 \boldsymbol{Z} + \bar{\boldsymbol{H}}_6, \quad \bar{\boldsymbol{H}}_6 \sim \mathcal{N}(\boldsymbol{0}, \sigma_\varphi^2 \boldsymbol{I}_{m-1}), \tag{24}$$

where $\mathrm{rank}(\bar{\boldsymbol{H}}_4) = m-1$. QR decomposition of $\bar{\boldsymbol{H}}_4$ can be written as

$$\bar{\boldsymbol{H}}_4 = \boldsymbol{Q}_{\bar{\boldsymbol{H}}_4}^{\mathrm{T}} \boldsymbol{R}_{\bar{\boldsymbol{H}}_4}, \tag{25}$$

where $\boldsymbol{Q}_{\bar{\boldsymbol{H}}_4}$ is an $(m-1)\times(m-1)$ orthogonal matrix, and $\boldsymbol{R}_{\bar{\boldsymbol{H}}_4}$ is an upper triangular matrix. Left-multiplying eq. (24) by $\boldsymbol{Q}_{\bar{\boldsymbol{H}}_4}$, we have

$$\bar{\boldsymbol{H}}_7 = \boldsymbol{R}_{\bar{\boldsymbol{H}}_4} \boldsymbol{Z} + \bar{\boldsymbol{H}}_8, \quad \bar{\boldsymbol{H}}_8 \sim \mathcal{N}(\boldsymbol{0}, \sigma_\varphi^2 \boldsymbol{I}_{m-1}), \tag{26}$$

where $\bar{\boldsymbol{H}}_7 = \boldsymbol{Q}_{\bar{\boldsymbol{H}}_4} \bar{\boldsymbol{H}}_2$, and $\bar{\boldsymbol{H}}_8 = \boldsymbol{Q}_{\bar{\boldsymbol{H}}_4} \bar{\boldsymbol{H}}_6$. So the floating resolution of DDIA can be written as

$$\hat{\boldsymbol{Z}} = (\boldsymbol{R}_{\bar{\boldsymbol{H}}_4}^{\mathrm{T}} \boldsymbol{R}_{\bar{\boldsymbol{H}}_4})^{-1} \boldsymbol{R}_{\bar{\boldsymbol{H}}_4}^{\mathrm{T}} \bar{\boldsymbol{H}}_2. \tag{27}$$

Furthermore, the fixed resolution of $\boldsymbol{Z}$ can be obtained by solving eq. (26), and this is equivalent to the following question:

$$\begin{aligned} &\min_{\boldsymbol{Z}} \|\bar{\boldsymbol{H}}_7 - \boldsymbol{R}_{\bar{\boldsymbol{H}}_4} \boldsymbol{Z}\|^2_{Q^{-1}_{\bar{\boldsymbol{H}}_7}}, \\ &\text{s.t.} \quad \boldsymbol{Z} \in \boldsymbol{Z}^{m-1}, \end{aligned} \tag{28}$$

where $\|\cdot\|^2_{Q^{-1}_{\bar{\boldsymbol{H}}_7}} = (\cdot)^{\mathrm{T}} Q^{-1}_{\bar{\boldsymbol{H}}_7}(\cdot)$. $Q^{-1}_{\bar{\boldsymbol{H}}_7}$ is the inverse of $\bar{\boldsymbol{H}}_7$'s covariance matrices. Given that

$$Q^{-1}_{\bar{\boldsymbol{H}}_7} = \sigma_\varphi^{-2} \boldsymbol{I}_{m-1}, \tag{29}$$

eq. (28) is equivalent to

$$\begin{aligned} &\min_{\boldsymbol{Z}} \|\bar{\boldsymbol{H}}_7 - \boldsymbol{R}_{\bar{\boldsymbol{H}}_4} \boldsymbol{Z}\|^2, \\ &\text{s.t.} \quad \boldsymbol{Z} \in \boldsymbol{Z}^{m-1}, \end{aligned} \tag{30}$$

where $\|\cdot\|^2 = (\cdot)^{\mathrm{T}}(\cdot)$. Also, eq. (30) can be divided into the following two parts:

$$\|\bar{\boldsymbol{H}}_7 - \boldsymbol{R}_{\bar{\boldsymbol{H}}_4} \boldsymbol{Z}\|^2 = \|\bar{\boldsymbol{H}}_7 - \boldsymbol{R}_{\bar{\boldsymbol{H}}_4} \boldsymbol{Z}\|^2 + \sum_{i=1}^{m} (\hat{z}_{i/I} - z_i)^2 / \sigma^2_{\hat{z}_{i/I}}, \tag{31}$$

where $\hat{z}_{i/I} = \hat{z}_i - \sum_{j=1}^{i-1} \sigma_{\hat{z}_{i/j|J}} \sigma^{-2}_{\hat{z}_{j|J}} (\hat{z}_{i/J} - z_j), I = 1, 2, \ldots, i-1$. $\hat{z}_{i/I}$ denotes the least-square estimation of the Ith DDIA under the constraint of z_1 to z_{i-1}. $\sigma^2_{\hat{z}_{i/I}}$ indicates the variance of $\hat{z}_{i/I}$. $\sigma_{\hat{z}_{i/j/J}}$ represents the covariance between $\hat{z}_i$ and $\hat{z}_{j/J}$. It is difficult to solve the right side of eq. (31) rapidly and accurately within GPS short observation time. At present, an effective method is LAMBDA, by means of which the fixed solution $\breve{\boldsymbol{Z}}$ of $\boldsymbol{Z}$ can be obtained [4]. The baseline vector $\boldsymbol{X}_K$ at epoch k can be achieved by inserting $\boldsymbol{Z} = \breve{\boldsymbol{Z}}$ into eq. (23). Modified LAMBDA method can also solve this problem. Though its computational efficiency is higher than LAMBDA, the results of the two algorithms are the same. As a result, the accuracy and reliability of DDIA are not improved [5]. This shows that the accuracy and reliability of DDIA in GPS are largely dependent on observations. So quantum ranging is introduced to improve the accuracy and reliability of DDIA.

2.3 GPS RTK aided by quantum ranging

Sketch of GPS RTK aided by quantum ranging is shown in Figure 1. The quantum beacon is established within user's short baseline range ($\leqslant$ 20 km). The beacon and user use the same GPS clock, and the quantum beacon transmits pulses strictly synchronized with GPS clock. It can be assumed the quantum

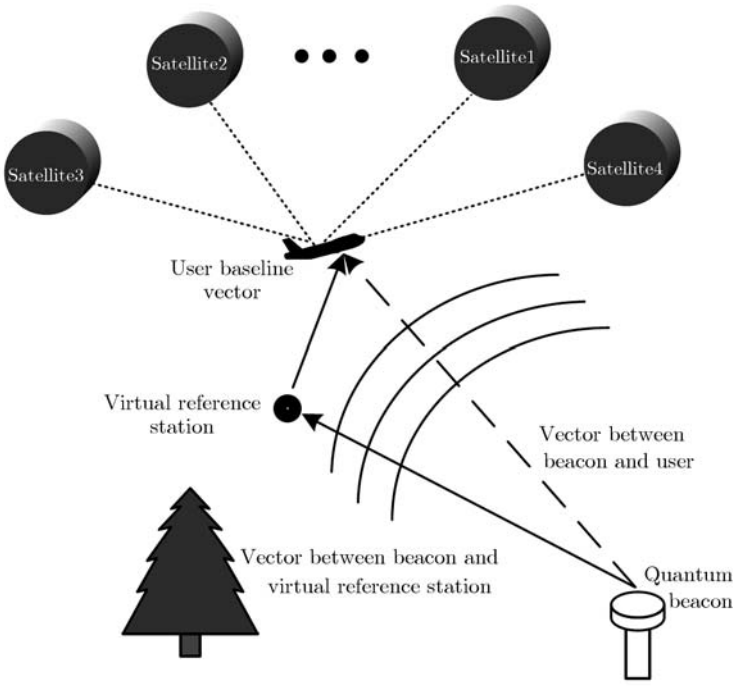

Figure 1 Sketch of GPS RTK aided by quantum ranging.

pulse with compression photons is C_p, and the entangled photon is E_t (total entanglement) and quantum efficiency is η_{en}. After photons r are emitted, the ranging accuracy can be achieved (see [6]),

$$\delta r = c\delta\tau C_p^{-1} E_t^{-1} r^{-0.5} \eta^{-0.5E_t}, \tag{32}$$

where c is light velocity, and $\delta\tau$ is a single unentangled photon timing error.

Let $\{x_{qt}, y_{qt}, z_{qt}\}$ denote the beacon station's earth core earth fixed (ECEF) coordinates. $\boldsymbol{X}'_K$ denotes distance vector between the beacon and virtual reference station. $\boldsymbol{X}''_K$ denotes distance vector between the beacon and user. From eq. (12) and Figure 1, we can find

$$\boldsymbol{X}''_K = \boldsymbol{X}_K + \boldsymbol{X}'_K, \tag{33}$$

where $\boldsymbol{X}'_K$ does not rely on user's observations, and

$$\boldsymbol{X}'_K = \begin{bmatrix} x_v(k) \\ y_v(k) \\ z_v(k) \end{bmatrix} - \begin{bmatrix} x_{qt} \\ y_{qt} \\ z_{qt} \end{bmatrix}, \qquad \boldsymbol{X}''_K = \begin{bmatrix} x_r(k) \\ y_r(k) \\ z_r(k) \end{bmatrix} - \begin{bmatrix} x_{qt} \\ y_{qt} \\ z_{qt} \end{bmatrix}.$$

$\boldsymbol{X}''_K$ in eq. (33) cannot be directly obtained in actual quantum ranging but the module of this vector (the distance between quantum beacon and user) can be obtained,

$$l'_K = l_K + \delta r_K, \tag{34}$$

where l_K indicates the true value of l'_K, and δr_K indicates the value of δr at epoch k. The relationship of $\boldsymbol{X}''_K$ and l_K is given by

$$\boldsymbol{X}''^{\mathrm{T}}_K \boldsymbol{X}''_K = l_K + \delta r''_K, \tag{35}$$

where $\delta r''_K$ indicates the estimation error of baseline length. Inserting eq. (33) into eq. (35), we have

$$(\boldsymbol{X}_K + \boldsymbol{X}'_K)^{\mathrm{T}} (\boldsymbol{X}_K + \boldsymbol{X}'_K) = l_K + \delta r''_K. \tag{36}$$

So it is easy to obtain the distance vector from virtual reference station to user after getting fixed solution $\breve{\boldsymbol{Z}}$ of DDIA by means of LAMBDA algorithm. Obviously, in this case, $\boldsymbol{X}_K$ corresponds to a certain specific

value of $\breve{\boldsymbol{Z}}$. The magnitude of $\delta r''_K$ reflects the magnitude of the error $\breve{\boldsymbol{Z}}$. So from eqs. (34) and (36), we can assume

$$\eta_K = |(\boldsymbol{X}_K + \boldsymbol{X}'_K)^{\mathrm{T}}(\boldsymbol{X}_K + \boldsymbol{X}'_K) - l'_K| \underset{\text{yes}}{\overset{\text{no}}{\lessgtr}} 3\sigma_{\delta r}, \tag{37}$$

where $\sigma_{\delta r}$ is the mean square error of δr. When η_K is more than $3\sigma_{\delta r}$, the value of $\breve{\boldsymbol{Z}}$ does not meet the requirements, and vice versa.

3 Simulation results

Based on the real RTK data distributed by the Delft University in Holland, 22 epochs data from 6 satellites are available after the elimination of satellites with elevation angles smaller than 10°. The C/A code observations, and L1 and L2 carrier phase observations are all included in the data.

The first epoch of observation is deemed as the reference one. The change of ECEF coordination of the 6 satellites is shown in Figure 2, and the corresponding change of geographic coordination is shown in Figure 3. PDOP of these 6 satellites related to the user is shown in Figure 4, where the change of PDOP within a few epochs is rather small, and this leads to the fact that more observation epochs should be included in order to get a reliable DDIA fixed solution. The L2 carrier phase observations are not employed in accordance with our initial assumptions. The virtual reference station's C/A code observations and carrier phase observations are deduced from the real data. Though it may not be the same as the real data, this will have little influence on our analytic results since all the observation error terms are set according to the real data. The satellite with the biggest elevation angle is selected as the reference satellite in both the positioning process and the DDIA fixed solution determination. The observation period is short, i.e. only 22 epochs are observed, and the reference satellite remains unchanged in the whole positioning process. Furthermore, the quantum pulses which use the entanglement and squeezing in ranging are simulated and the range between user and quantum beacon is always smaller than 80 km throughout all the epochs.

The positioning simulation is taken under the following three scenarios: 1) positioning without any ranging aided; 2) positioning with classical ranging aided. Here the ranging precision is deemed to be equal to the precision of the double differenced C/A code observation; 3) ranging with high precision quantum pulse aided (2-photon squeezing, a maximum of 5 photon entanglement, 98% transition efficiency). The estimation results of baseline vector between user and virtual reference station in the three scenarios are shown in Figures 5–7. So DDIA can be fixed within a few observation epochs when additional ranging observation is included, especially with the help of high precision quantum ranging.

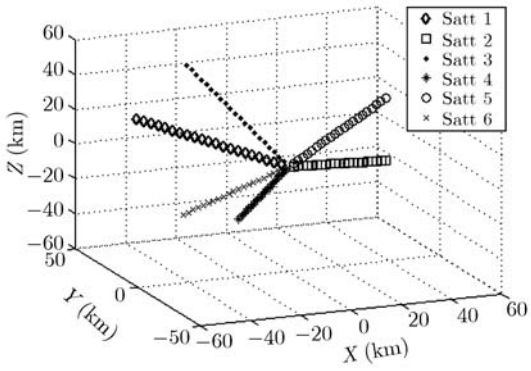

Figure 2 The change of GPS satellites' ECEF coordination at different epochs.

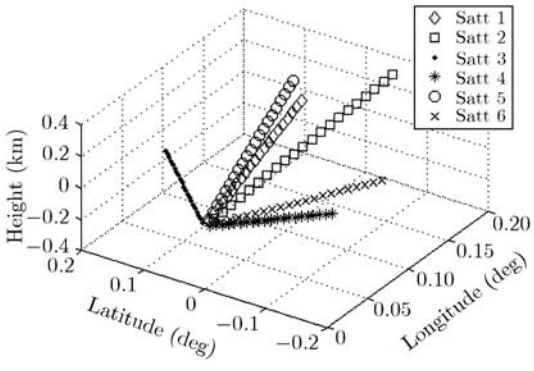

Figure 3 The change of GPS satellites' geography at different epochs.

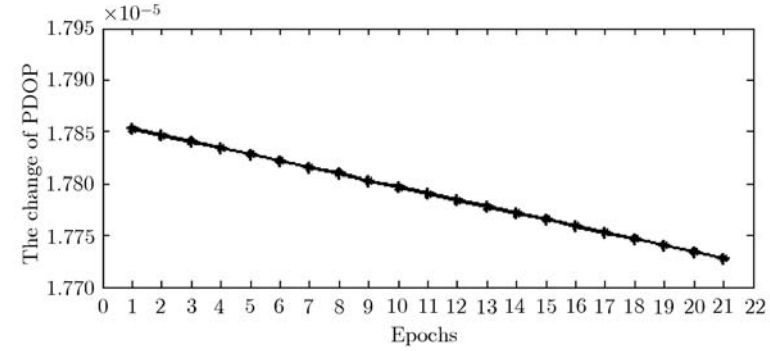

Figure 4 The change of PDOP at different epochs.

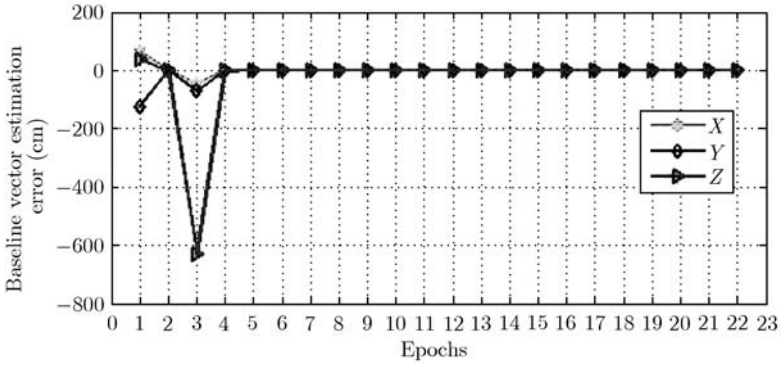

Figure 5 Baseline vector estimation errors without any ranging aided.

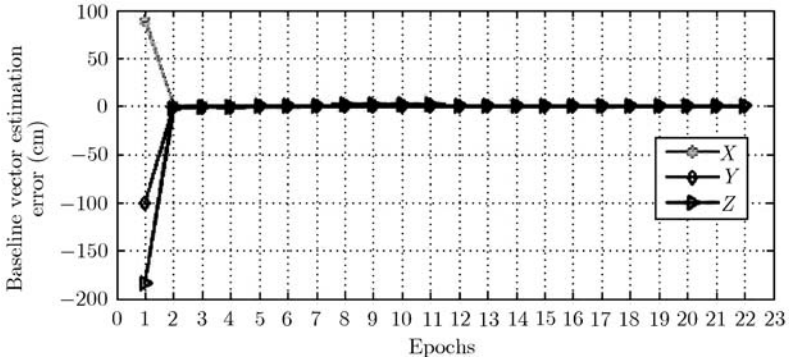

Figure 6 Baseline vector estimation errors with classical ranging aided.

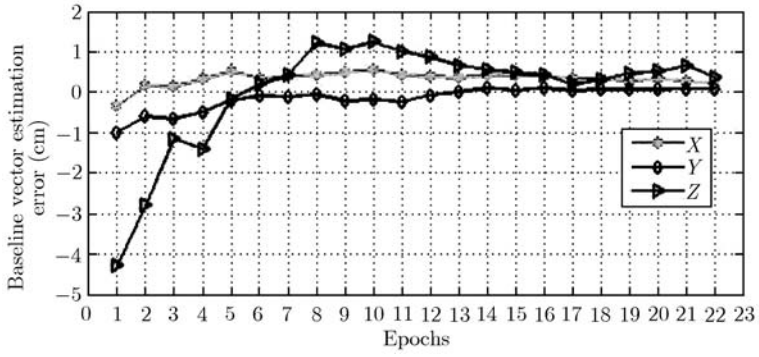

Figure 7 Baseline vector estimation errors with the aid of quantum.

4 Conclusions

(1) The computation burden can be reduced effectively when GPS' C/A code observations are smoothed by the single differenced phase observations without the dilution of the positioning precision.

(2) QR factorization can be used to get a numerically stable DDIA float solution in GPS network RTK. Householder transformation can be used instead of double differenced method to maintain the independence of C/A code observations and that of carrier phase observations. It is helpful for the DDIA fixed solution.

(3) The number of DDIA candidates can be reduced when the high precision quantum ranging observation is also included. This will provide the possibility to fix the DDIA within a relatively short observation period and to repair cycle slip within a few epochs.

Acknowledgements

This work was supported by the National Natural Science Foundation of China (Grant No. 60678018).

References

1 NovAtel Inc. Introducing NovAtel's New AdVance RTK NovAtel Technical Report, 2000
2 Raquet J, Lachapelle G. RTK positioning with multiple reference stations. GPS World, 2001, 12: 48–53
3 Chang X W, Paige C C, Yin L. Code and carrier phase based short baseline GPS positioning: computational aspects. GPS Solution, 2005, 9: 72–83
4 Teunissen P J, Tiberius C C. The least-squares ambiguity decorrelation adjustment: its performance on short GPS baselines and short observation spans. J Geodesy, 1997, 71: 589–602
5 Chang X W, Yang X, Zhou T. MLAMBDA: A modified LAMBDA method for integer least-squares estimation. J Geodesy, 2006, 79: 552–565
6 Giovannetti V, Lloyd S, Maccone L. Quantum enhanced positioning and clock synchronization. Nature, 2001, 412: 417–419
7 Giovannetti V, Lloyd S, Maccone L. Quantum-enhanced measurements: beating the standard quantum limit. Science, 2004, 306: 1330–1334
8 Giovannetti V, Lloyd S, Maccone L. Positioning and clock synchronization through entanglement. Phys Rev A, 2001, 88: 183602-1—183602-4
9 Giovannetti V, Lloyd S, Maccone L. Quantum positioning system. In: Proceedings of the 8th Rochester Conference on Coherence and Quantum Optics. New York: Kluwer Academic/Plenum Publishers, 2003. 323–324
10 Thomas B B. Quantum positioning system. In: 36th Annual Precise Time and Time Interval (PTTI) Meeting, Naval Observatory. Washington DC, 2005. 423–427
11 Yang C Y, Wu D W, Lu Y E, et al. Phase-smoothed pseudo-range algorithm based on complementary Kalman filtering (in Chinese). J Air Force Eng Univ (Nat Sci Ed), 2008, 9: 40–45